ACS Catalysis

Research Article

pubs.acs.org/acscatalysis

# Influence of Electrolyte Composition and pH on Platinum Electrochemical and/or Chemical Dissolution in Aqueous Acidic Media

Yoshihisa Furuya,[†,‡] Tetsuya Mashio,[†] Atsushi Ohma,[†] Min Tian,[‡] Farhad Kaveh,[‡] Diane Beauchemin,[‡] and Gregory Jerkiewicz*[,‡]

[†]Nissan Research Center, Nissan Motor Company, 1-Natsushima Cho, Yokosuka, Kanagawa 237-8523, Japan

[‡]Department of Chemistry, Queen's University, 90 Bader Lane, Kingston, Ontario K7L 3N6, Canada

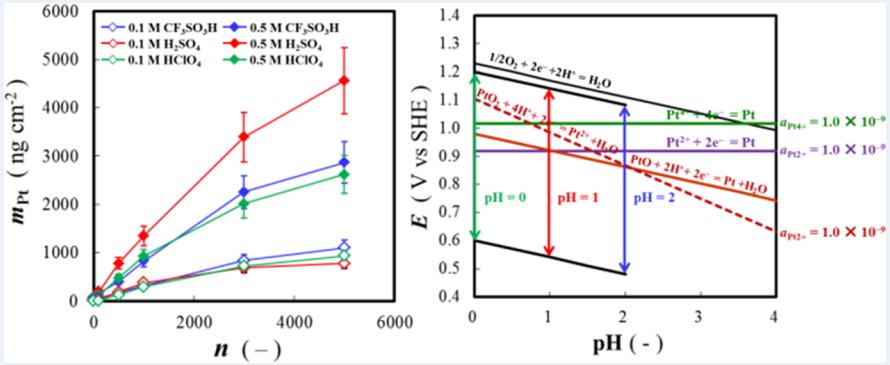


**ABSTRACT:** Comprehension of the impact of electrolyte nature and concentration on Pt degradation is essential for the improvement of durability of catalyst layers (CLs), which are the heart of polymer electrolyte membrane fuel cells (PEMFCs). Electrochemical and chemical dissolution of polycrystalline Pt in aqueous $CF_3SO_3H$, $H_2SO_4$, and $HClO_4$ solutions of different concentrations ($c$ = 0.1 and 0.5 M) upon potential switching and holding in the 0.60−1.20 V versus RHE range is analyzed using inductively coupled plasma mass spectroscopy. This potential range mimics the conditions encountered in operating PEMFCs. Trifluoromethanesulfonic acid ($CF_3SO_3H$) is employed because it is the smallest fluorinated sulfonic acid and can serve as a model molecule. Degradation of Pt in $H_2SO_4$ and $HClO_4$ solutions is examined for comparative analysis. The results reveal that the electrolyte concentration has a significant impact on Pt electrochemical and chemical dissolution. The amount of dissolved Pt in 0.1 M solutions of $CF_3SO_3H$, $H_2SO_4$, and $HClO_4$ is practically the same and lower than that in analogous 0.5 M solutions. However, the amount of dissolved Pt in 0.5 M $H_2SO_4$ solution is greater than that in 0.5 M solutions of $CF_3SO_3H$ or $HClO_4$. The influence of anion nature and pH on Pt dissolution is examined in 0.1 and 0.5 M $HClO_4$ solutions without and with $1.0 \times 10^{-2}$ M $H_2SO_4$ addition. The results show that under these conditions the anion nature has no or negligible impact on Pt dissolution, but pH significantly affects the process. An analysis of potential versus pH diagrams (Pourbaix diagrams) for acid solutions of different pH values suggests that Pt degradation (with the formation of $Pt^{2+}$(aq) and $Pt^{4+}$(aq)) might proceed through both electrochemical and chemical pathways.

**KEYWORDS:** *fuel cells, platinum electro-dissolution, platinum oxide, potential cycling, inductively coupled plasma mass spectrometry*

## INTRODUCTION

Polymer electrolyte membrane fuel cells (PEMFCs) are promising sources of electrical power for zero emission vehicles (ZEVs). Although numerous research efforts have been dedicated to the development of PEMFCs over the past 10 years, further cost reduction and improvement of performance and durability are key issues that need to be addressed in order to achieve mass production of affordable fuel cell electric vehicle (FCEVs).[1,2] Catalyst layers (CLs), which are one of the main components of fuel cells, comprise Pt nanoparticles (Pt-NPs) that are covered with ionomer (e.g., Nafion) and reside on a carbon support; the Pt-NPs are the electrocatalysts at which the hydrogen oxidation reaction (HOR) and oxygen reduction reaction (ORR) occur. Decrease in the size of Pt-NPs is one of the approaches for reducing Pt loading, but the diminished particles' size increases their surface Gibbs energy and reduces their stability; these interrelated phenomena lead to gradual degradation of Pt-NPs.[3−8] Consequently, Pt-NPs are more prone to chemical and electrochemical dissolution than bulk Pt materials, and their degradation during the operation of PEMFCs is a very important technological issue that requires resolution.

Received: October 16, 2014
Revised: March 11, 2015
Published: March 16, 2015




DOI: 10.1021/cs5016035
ACS Catal. 2015, 5, 2605−2614

During accelerating, decelerating, idling, start-up, and shut-down (repetitive accelerating and decelerating is often referred to as load cycling), automotive fuel cells operate at relatively high potentials, at which the Pt surface undergoes partial or complete electro-oxidation.[9−12] The Pt surface oxide influences the lifetime of Pt-NPs as oxidized surfaces reveal different corrosion properties than metallic ones; it can function as a protective (passive) layer on metallic Pt or can facilitate Pt chemical and/or electrochemical dissolution, if the Pt oxide is thermodynamically less stable than metallic Pt.[3,13−15] Such a behavior can be related to the surface oxide structure, which can adopt either the form of chemisorbed O ($O_{chem}$) residing on Pt surface or the form of $PtO_{quasi\text{-}3D\ lattice}$ comprising $Pt^{2+}$ and $O^{2-}$ species. The transition from $O_{chem}$ to $PtO_{quasi\text{-}3D\ lattice}$ occurs through a structural transformation colloquially referred to as a place-exchange process.[5,6,13,16−21] Because the composition and structure of Pt surface oxide affect the rate of chemical and/or electrochemical dissolution of Pt-NPs, it is important to analyze the process in relation to polarization conditions as well as the electrolyte composition and pH. The structural nature of the Pt surface oxide is important because it affects the mechanism and rate of its dissolution.

Several studies deal with Pt dissolution upon potential cycling in relation to various experimental parameters, such as the upper and lower potential limit ($E_U$ and $E_L$, respectively),[13,15,17−19,22,23] the potential scan rate ($s$),[13,19,24] temperature ($T$),[13,24] presence of gaseous species,[16,25,26] the electrolyte composition and pH,[27] and the types of Pt materials.[28] $E_U$ and $E_L$ are possibly the two most important experimental parameters the impact of which needs to be examined in order to understand the mechanistic and kinetic aspects of Pt dissolution during the operation of FCEVs. Several groups reported that Pt dissolution becomes more pronounced when $E_U$ is raised from 1.10 to 1.20 V (for $E_L$ = const).[13,15,17,22] This observation supports the notion that the structural transformation that develops $PtO_{quasi\text{-}3D\ lattice}$ exposes oxidized Pt atoms (in the form of $Pt^{2+}$) which are more prone toward dissolution that $Pt-O_{chem}$. It was also reported that Pt dissolution is affected by $E_L$ (for $E_U$ = const), which in some instances might be low enough to drive electrodeposition of previously dissolved Pt species.[13,15,17,22] It is important to add that there is indisputable evidence that Pt undergoes dissolution during both anodic and cathodic transients in typical cyclic-voltammetry (CV) experiments.[18,19]

The anion constituting an acidic electrolyte can influence Pt chemical and electrochemical dissolution through its interaction with the Pt surface and also by affecting the equilibrium constant of the dissolved $Pt^{z+}$-containing complex compound, whose nature remains unknown. In CLs, Nafion acts both as a solid electrolyte and a separator; due to its high acidity and direct contact with Pt-NPs, it can impact Pt dissolution. The chemical environment experienced by Pt-NPs being in direct contact with the Nafion ionomer is different from that encountered in conventional acidic media: the proton concentration is high, and the anion (here sulfonic group) adsorbed on the Pt surface is immobile due to its polymeric nature (or has very limited mobility); its interactions with Pt is reported to be weak.[29−32] Although numerous papers report on Pt dissolution in conventional acidic media (e.g., aqueous $H_2SO_4$ and $HClO_4$ solutions), knowledge of the influence of electrolyte nature on the process is very limited. Trifluoromethanesulfonic acid ($CF_3SO_3H$, abbreviated as TFMSA) is the smallest fluorinated sulfonic acid and can serve as a suitable molecular model of a strong, fluorinated acid.[33−35] The strength of anion interaction with the Pt surface in $CF_3SO_3H$ is weaker than that in $H_2SO_4$.[36−39] Consequently, if the anion constituting the electrolyte were to affect Pt dissolution, results obtained in aqueous $CF_3SO_3H$ solutions should differ from analogous data obtained in other conventional electrolytes (e.g., $H_2SO_4$ or $HClO_4$). Thus, in order to better understand the mechanism and kinetics of Pt dissolution, and in particular the impact of electrolyte composition, it is necessary to study the process in electrolytes having different anion types, different electrolyte concentrations and pH values.[19]

In this contribution, we report on a study of Pt electrochemical and chemical dissolution upon potential switching and holding in aqueous $CF_3SO_3H$, $H_2SO_4$, and $HClO_4$ solutions. The process is examined in relation to the electrolyte nature and its concentration with the objective of determining whether the anion nature and the electrolyte pH have any impact on the process. The amount of dissolved Pt present in the electrolytes is analyzed using inductively coupled plasma mass spectrometry. The results are discussed in the framework of potential versus pH diagrams for Pt.

## EXPERIMENTAL SECTION

**Electrodes, Electrolytes, and Electrochemical Cells.** The working (WE) and counter (CE) electrodes were made of Pt foil; each was spot-welded to a Pt wire that was sealed in a glass tube. The working and counter electrodes were degreased in acetone under reflux followed by rinsing with ultrahigh purity ethanol. Then, they were cleaned in concentrated $H_2SO_4$ for 24 h and rinsed several times (at least 10 times) with ultrahigh purity water (MilliPore, Milli-Q3; $\rho \geq 18.2$ MΩ cm). The geometric dimensions of WE and CE were 1.55 cm × 1.65 cm. The electrochemically active surface area ($A_{ecsa}$) of the WE electrode was determined from the charge of the underpotential deposition of H (UPD H).[40] The electrode's roughness factor ($R = A_{ecsa}/A_{geom}$, where $A_{geom}$ is the geometric surface area) was found to be ca. 1.7. The reference electrode was polycrystalline Pt coated with Pt black placed in the same electrolyte as that in the WE compartment but in a separate compartment through which $H_2(g)$ ($p_{H_2}$ = 1.0 atm) presaturated with water vapor was passed; it served as a reversible hydrogen electrode (RHE). The RHE compartment was electrolytically connected to the WE compartment by means of a Luggin capillary. All potentials measured experimentally and referred to in this paper are expressed with respect to RHE. All electrochemical experiments were conducted using a three-compartment cell. The separation of the WE and CE compartments by means of a Nafion 211 membrane was necessary in order to eliminate any influence of dissolved Pt originating from CE.[13] A new Nafion membrane was used in each experiment.

High purity aqueous electrolyte solutions were prepared from concentrated $CF_3SO_3H$ (ReagentPlus, Sigma-Aldrich >99%), $H_2SO_4$ (Fluka, > 95%), $HClO_4$ (Sigma-Aldrich, > 70%), and ultrahigh purity water (MilliPore, Milli-Q3; its resistivity was $\rho \geq 18.2$ MΩ cm). The concentrated acids were used as received without any further purification. The glassware was cleaned using well-established and widely accepted procedures.[41] Ultrahigh purity $N_2(g)$ presaturated with water vapor was passed through the electrolyte in the WE and CE compartments. The attainment of a CV profile characteristic of


DOI: 10.1021/cs5016035
ACS Catal. 2015, 5, 2605−2614

a clean system (the electrodes, electrolyte, and cell) and the stability and reproducibility of CV profiles over prolonged periods of time were carefully verified as a measure of the purity of the entire experimental setup. In addition, the value of $A_{ecsa}$ was maintained constant to within 3% of its initial value confirming that the system was impurity-free. All experiments were conducted at room temperature ($T$ = 293 ± 1 K).

**Electrochemical Experiments and Electrolyte Solution Collection for Analysis.** After assembling the experimental setup, the WE and CE compartments were purged with ultrahigh purity $N_2$(g) for ca. 30−60 min. The electrolyte solution in the WE compartment was agitated using a magnetic stirrer. The working electrode was cycled 10 times in the 0.05−1.40 V range at a potential scan rate of $s$ = 50 mV $s^{-1}$. Then, an aliquot of ca. 1.0 mL of electrolyte was collected from the WE compartment; it served as a blank and refers to the zeroth potential cycle. Repetitive potential switching (potential stepping) and holding between the lower and upper potential limits ($E_L$ and $E_U$) was commenced immediately afterward (Figure 1), while the electrolyte was continuously agitated

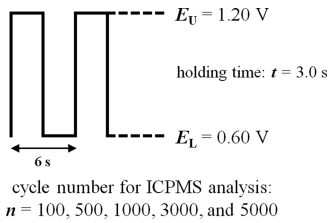


**Figure 1.** Schematic representation of the potential switching and holding program employed in Pt dissolution studies; the upper and lower potential limits are $E_U$ = 1.20 V and $E_L$ = 0.60 V, respectively; the potential scan (switch) rate between $E_U$ and $E_L$ is $s$ = 7500 mV $s^{-1}$; the holding time at $E_U$ and $E_L$ is $t$ = 3.0 s.

using a magnetic stirrer; one complete switching and holding cycle refers to $E_L \rightarrow E_U \rightarrow E_L$. A square-wave potential program was used as shown in Figure 1; the lower and upper potential limits were $E_L$ = 0.60 V and $E_U$ = 1.20 V, respectively. The potential switching between $E_L$ and $E_U$ was not instantaneous and corresponded to an extremely steep ramp and a potential scan rate of $s$ = 7500 mV $s^{-1}$. Because it took 80 ms for the applied potential to switch between $E_L$ and $E_U$, the potential profile was considered to be practically square-shaped; following the switching, the potential was held at $E_L$ and $E_U$ for a holding time of $t$ = 3.0 s. An aliquot of ca. 1.0 mL of electrolyte was collected at the following numbers ($n$) of potential switching and holding cycles: 100th, 500th, 1000th, 3000th, and 5000th. The electrolyte solution volume was maintained constant by adding ca. 1.0 mL of fresh electrolyte right after each electrolyte aliquot collection. The total volume of electrolyte in the WE compartment was ca. 60 mL. Each electrolyte sample was carefully weighed using an analytical balance. Accurate mass and volume determination of each sample was required in order to perform quantitative data analysis. Following mass and volume determination, each electrolyte aliquot was carefully diluted 5-fold using ultrahigh purity water prior to submission for inductively coupled plasma mass spectrometry measurements.[13]

**Inductively Coupled Plasma Mass Spectrometry Analysis.** Inductively coupled plasma mass spectrometry (ICP-MS) analysis was performed using a Varian 820-MS instrument with a detection limit of 10 ppt. Standard solutions for ICP-MS measurements were prepared by dilution of Pt stock solution (10000 μg/mL in 10% HCl, SCP Science) in 5-fold diluted electrolyte solution and were measured in order to prepare a calibration curve. The sample introduction system was then flushed with the blank solution until the counts reached the level comparable to that prior to measurements. The samples were then analyzed in the sequence of collection.[13]

**Determination of the Amount of Pt Oxide Expressed as Chemisorbed Oxygen Surface Coverage.** A surface oxide was grown on polycrystalline Pt electrode under potentiostatic conditions by applying a constant polarization potential of $E_p$ = 1.20 V at $T$ = 293 K for a controlled polarization time in the $1.0 \times 10^0 \leq t_p \leq 1.0 \times 10^4$ s range. In each separate experiment, a surface oxide formed by potentiostatic polarization was subsequently reduced in a single negative-going CV transient at a potential scan rate of $s$ = 50 mV $s^{-1}$. All CV oxide-reduction profiles show one feature, the so-called OC1 peak, which corresponds to the reduction of surface PtO to metallic Pt, as described elsewhere.[42] Such acquired oxide reduction CV profiles were integrated in order to determine oxide charge density ($q_{ox}$) values. The amount of PtO, which can also be expressed as a surface coverage ($\theta_O$) of chemisorbed oxygen ($O_{chem}$) was determined by dividing the $q_{ox}$ values by the charge density associated with the formation of one monolayer of $O_{chem}$ on polycrystalline Pt, thus by $q_{ox,1\ ML}$ = 440 μC $cm^{-2}$. Potential switching from 0.60 to 1.20 V followed by holding for 3.0 s results in the formation of a thin surface oxide layer the charge density of which is $q_{ox}$ = 330 ± 10 μC $cm^{-2}$. This charge density corresponds to the equivalent $O_{chem}$ coverage of $\theta_O$ = 0.75.

## RESULTS AND DISCUSSION

**Platinum Dissolution in Aqueous $CF_3SO_3H$, $H_2SO_4$, and $HClO_4$ Solutions.** Figure 2 presents two graphs for a polycrystalline Pt electrode in aqueous $CF_3SO_3H$ (blue line), $H_2SO_4$ (red line), and $HClO_4$ (green line) solutions obtained at $s$ = 50 mV $s^{-1}$ and $T$ = 293 K; the graphs A and B are for 0.1 and 0.5 M solutions, respectively. The pH values of these solutions are as follows: (i) 0.1 M $CF_3SO_3H$, pH = 1.1; (ii) 0.5 M $CF_3SO_3H$, pH = 0.44; (iii) 0.1 M $H_2SO_4$, pH = 1.5; (iv) 0.5 M $H_2SO_4$, pH = 1.1; (v) 0.1 M $HClO_4$, pH = 1.1; and (vi) 0.5 M $HClO_4$, pH = 0.42. The CV transients reveal the usual features corresponding to the electro-adsorption and electro-desorption of under-potential deposited H ($H_{UPD}$) and the formation and reduction of Pt surface oxide; the shape of the CV profiles demonstrates that the system (electrodes, electrolyte, cell) is impurity-free.

The onset potential of $H_{UPD}$ electro-adsorption in the $H_2SO_4$ solution is slightly lower than that in the $CF_3SO_3H$ and $HClO_4$ solutions. The CV profiles obtained in the $CF_3SO_3H$ and $HClO_4$ solutions are similar suggesting that the anions experience similar interactions with the Pt surface. In addition, the CV peaks for UPD H in the $CF_3SO_3H$ and $HClO_4$ solutions have lower current density ($j$) values than those in the $H_2SO_4$ solution; these variances are attributed to different strengths of anion interactions with the Pt electrode.

Figure 3 presents the amount of dissolved Pt ($m_{Pt}$ in ng $cm^{-2}$) versus the potential switch cycle number ($n$) for repetitive potential switching and holding between 0.60 and 1.20 V through the application of a square-shaped wave at $T$ = 293 K in aqueous $CF_3SO_3H$ (blue diamonds), $H_2SO_4$ (red diamonds), and $HClO_4$ (green diamonds) solutions having two


DOI: 10.1021/cs5016035
ACS Catal. 2015, 5, 2605−2614

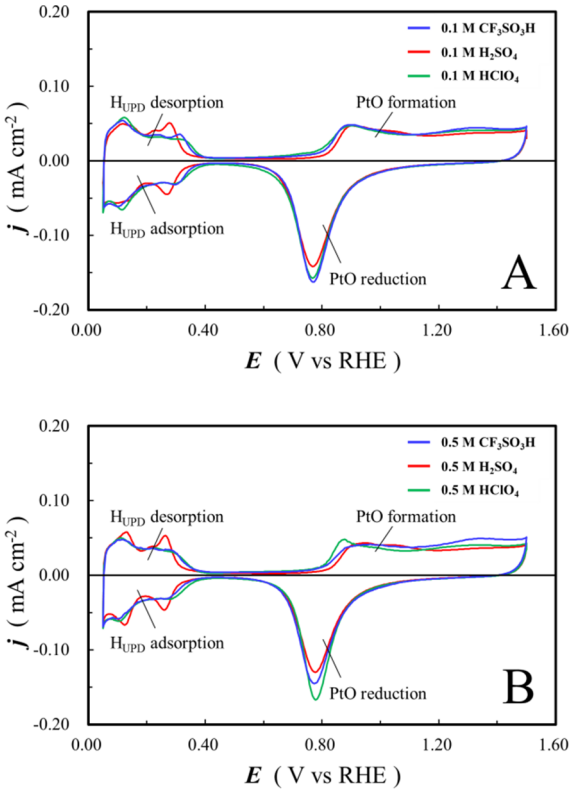


**Figure 2.** Two sets of CV profiles for the polycrystalline Pt electrode in aqueous $CF_3SO_3H$ (blue line), aqueous $H_2SO_4$ (red line), and aqueous $HClO_4$ (green line) obtained at $s$ = 50 mV $s^{-1}$ and $T$ = 293 K. Graphs **A** and **B** refer to 0.1 and 0.5 M solutions, respectively.

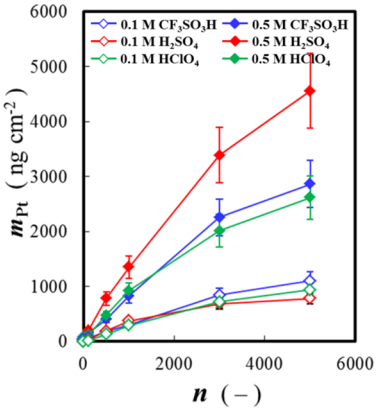


**Figure 3.** Amount of dissolved Pt ($m_{Pt}$) versus the potential switch cycle number ($n$) for repetitive potential switching and holding between 0.60 and 1.20 V at $T$ = 293 K in aqueous $CF_3SO_3H$ (blue diamonds), $H_2SO_4$ (red diamonds), and $HClO_4$ (green diamonds) solutions having 0.1 M (open diamonds) and 0.5 M (filled diamonds) concentrations.

different concentrations ($c$), namely, $c$ = 0.1 and 0.5 M. The amount of dissolved Pt is cumulative and refers to the total amount in the electrolyte solutions. The results presented in Figure 3 can be summarized as follows: (i) in the case of 0.1 M solutions (open diamonds), the amount of dissolved Pt is practically the same in the three electrolytes; (ii) in the case of 0.5 M solutions (filled diamonds), the amount of dissolved Pt in $H_2SO_4$ solution has higher values than in the other two solutions; (iii) the amount of dissolved Pt in the 0.5 M $H_2SO_4$ solution is ca. 4−5 times higher than that in the 0.1 M $H_2SO_4$ solution; (iv) the amount of dissolved Pt in the 0.5 M $CF_3SO_3H$ and $HClO_4$ solutions is ca. 3−4 times higher than that in 0.1 M $CF_3SO_3H$ and $HClO_4$ solutions. Here, we report for the first time experimental data for Pt dissolution in $CF_3SO_3H$ solutions brought about by repetitive potential switching and holding under conditions that mimic operating FCEVs. Our results show that for a given acid concentration, the amount of dissolved Pt in the $CF_3SO_3H$ solution is practically the same as that in the $HClO_4$ solution. The significantly higher dissolution of Pt in the 0.5 M $H_2SO_4$ solution versus the 0.5 M $CF_3SO_3H$ and $HClO_4$ solutions is unexpected, and as we demonstrate in a subsequent section, it cannot be easily associated with the anion adsorption on Pt. Although at present the exact nature of the $Pt^{2+}$- and $Pt^{4+}$-containing complex compounds remains unknown, it is feasible that the higher dissolution of Pt in the 0.5 M $H_2SO_4$ solution is related to the equilibrium constants of $Pt^{2+}$- and $Pt^{4+}$-containing complex compounds. The data also show that the electrolyte pH has a major impact on Pt dissolution.[19]

**Dissolution in Aqueous $HClO_4$ Solution without and with $H_2SO_4$ Addition.** $HClO_4$ is accepted to be a non-adsorbing or weakly adsorbing electrolyte and is often used in interfacial electrochemistry and electrocatalysis studies for a comparative analysis with a strongly adsorbing electrolyte (e.g., $H_2SO_4$). In this study, we examine Pt dissolution in 0.1 and 0.5 M aqueous $HClO_4$ solutions without and with an addition of $H_2SO_4$ (the concentration of $H_2SO_4$ after the addition is 1.0 × $10^{-2}$ M) with the objective of examining the impact of the anion nature on the process. Figure 4 presents CV profiles for a

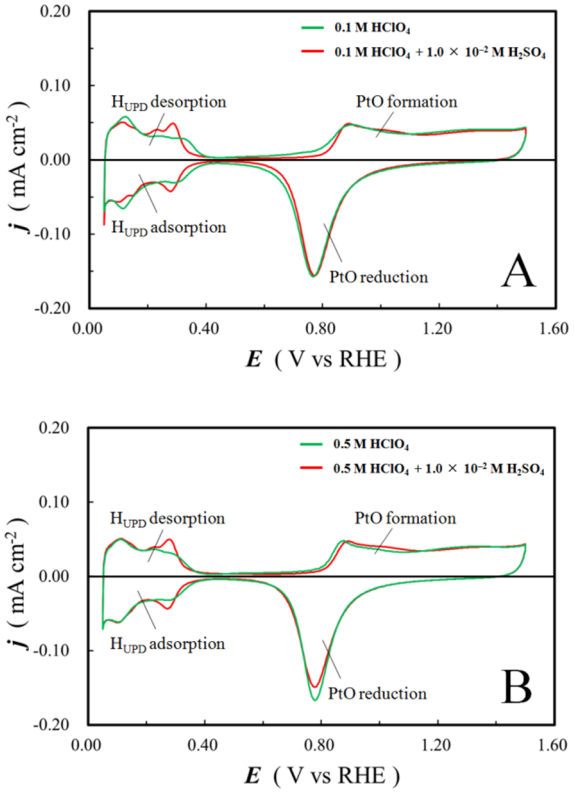


**Figure 4.** Two sets of CV profiles for the polycrystalline Pt electrode in aqueous $HClO_4$ solution without (green line) and with (red line) addition of $H_2SO_4$ obtained at $s$ = 50 mV $s^{-1}$ and $T$ = 293 K. Graphs **A** and **B** refer to 0.1 and 0.5 M solutions, respectively. After the addition, the $H_2SO_4$ concentration is 1.0 × $10^{-2}$ M.



DOI: 10.1021/cs5016035
ACS Catal. 2015, 5, 2605−2614

polycrystalline Pt electrode in $HClO_4$ solutions without (green line) and with (red line) addition of $H_2SO_4$ obtained at $s$ = 50 mV $s^{-1}$ and $T$ = 293 K; the graphs A and B in Figure 4 refer to 0.1 and 0.5 M $HClO_4$ solutions, respectively. The CV profiles reveal that the addition of $H_2SO_4$ shifts the CV peaks associated with UPD H toward slightly less-positive potential values and makes them sharper. The same qualitative features are observed in both the 0.1 and 0.5 M $HClO_4$ solutions. Because UPD H and anion electro-adsorption can overlap over a very narrow potential range (this is limited to small coverages of $H_{UPD}$ and anion), the CV feature in the low $H_{UPD}$ coverage region is influenced by the anion. Because $HSO_4^-$ and $SO_4^{2-}$ are strongly adsorbing species, the potential shift and the increase in the peak sharpness can be attributed to the anion interaction with the Pt surface. One could argue that higher concentrations of $H_2SO_4$ could be employed to further examine the anion effect, but it is well-established that the anion coverage reaches saturation already at concentrations in the 0.001−0.01 M range.[43]

Figure 5 presents the amount of dissolved Pt ($m_{Pt}$ in ng $cm^{-2}$) versus the potential switch cycle number ($n$) for

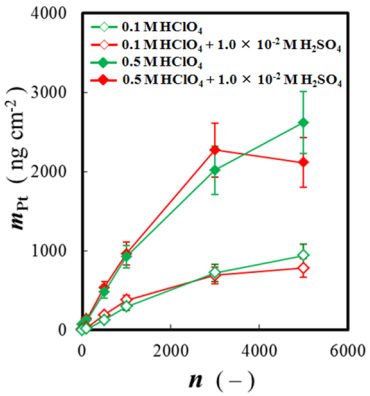


**Figure 5.** Amount of dissolved Pt ($m_{Pt}$) versus the potential switch cycle number ($n$) for repetitive potential switching and holding between 0.60 and 1.20 V at $T$ = 293 K in 0.1 and 0.5 M aqueous $HClO_4$ solution without (green diamonds) and with (red diamonds) the addition of $H_2SO_4$ (the concentration of $H_2SO_4$ after the addition is 1.0 × $10^{-2}$ M). The open and filled diamonds refer to 0.1 and 0.5 M aqueous $HClO_4$ solutions, respectively.

repetitive potential switching and holding between 0.60 and 1.20 V at $T$ = 293 K in 0.1 and 0.5 M aqueous $HClO_4$ solution without (green diamonds) and with (red diamonds) the addition of $H_2SO_4$ (the concentration of $H_2SO_4$ after the addition is 1.0 × $10^{-2}$ M). The amount of dissolved Pt is cumulative and refers to the total amount in the electrolyte solutions. The results demonstrate that the addition of $H_2SO_4$ does not alter the amount of dissolved Pt. The same qualitative behavior is observed for both the 0.1 and 0.5 M $HClO_4$ solutions. Also, the amount of dissolved Pt in the 0.5 M $HClO_4$ solution is higher than that in the 0.1 M $HClO_4$ solution irrespective of the presence of $H_2SO_4$. It is important to add that the proton activity in $HClO_4$ with the addition of $H_2SO_4$ is almost the same as that in the $HClO_4$ solution alone, because the concentration of $H_2SO_4$ is at least an order of magnitude smaller than the concentration of $HClO_4$. Thus, the addition of $H_2SO_4$ does not modify the overall proton activity (or modifies it only slightly) but replaces weakly adsorbing anions with strongly adsorbing ones. The results presented in Figure 5 lead to the conclusion that the anion has no or negligible impact on Pt dissolution, but the pH significantly affects the process.

We also examined the influence of anion nature on PtO formation, because the amount of PtO (here expressed as an oxide charge density, $q_{ox}$) present on a Pt electrode can affect Pt dissolution, provided that the dissolved Pt originates from PtO either during its formation or during its reduction.[18,19] Figure 6

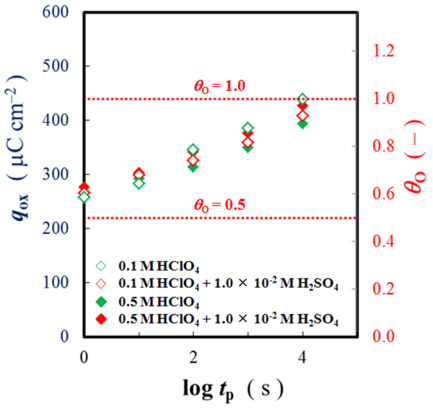


**Figure 6.** Oxide charge density ($q_{ox}$) versus log $t_p$ plots (for 1.0 × $10^0$ ≤ $t_p$ ≤ 1.0 × $10^4$ s) for Pt surface oxide growth at $E_p$ = 1.20 V and $T$ = 293 K in 0.1 and 0.5 M aqueous $HClO_4$ solutions without (green diamonds) and with (red diamonds) the addition of $H_2SO_4$ (the concentration of $H_2SO_4$ after the addition is 1.0 × $10^{-2}$ M). The open and filled diamonds refer to 0.1 and 0.5 M aqueous $HClO_4$ solutions, respectively.

presents $q_{ox}$ versus log $t_p$ plots (1.0 × $10^0$ ≤ $t_p$ ≤ 1.0 × $10^4$ s) for $E_p$ = 1.20 V and $T$ = 293 K in 0.1 and 0.5 M aqueous $HClO_4$ solutions without (green diamonds) and with (red diamonds) addition of $H_2SO_4$ (the concentration of $H_2SO_4$ after the addition is 1.0 × $10^{-2}$ M). As expected, the results demonstrate that $q_{ox}$ increases with a rise in $t_p$ but the values of $q_{ox}$ in the four electrolytes differ by only ca. 7−10% (the difference in $q_{ox}$ values is close to the experimental uncertainty of $q_{ox}$ determination) throughout the entire $t_p$ range, indicating that the anion nature and electrolyte concentration have little impact on the PtO development. The values of $q_{ox}$ are consistently in the 250−440 $\mu$C $cm^{-2}$ range; thus, the $O_{chem}$ coverage varies from $\theta_O$ = 0.57 to 1.0. Above, it is explained that in the case of polycrystalline Pt structural transformation from $O_{chem}$ to $PtO_{quasi\text{-}3D\ lattice}$ commences when $O_{chem}$ reaches the coverage of ca. $\theta_O$ = 0.5 and the surface oxide is entirely transformed when $\theta_O$ = 1.0. Thus, $q_{ox}$ = 250 $\mu$C $cm^{-2}$ corresponds to Pt oxide containing mainly $O_{chem}$ and $Pt_{surf}$ species ($Pt_{surf}$ refers to a surface Pt atom), while $q_{ox}$ = 440 $\mu$C $cm^{-2}$ corresponds to an entirely transformed surface oxide layer comprising $Pt^{2+}$ and $O^{2-}$ species. Because the values of $q_{ox}$ obtained in the four electrolytes are practically the same (within the experimental uncertainty) and correspond to both an oxide layer prior to and after the structural transformation, we can conclude that the anion nature and its concentration have practically no impact on the surface oxide growth on Pt. It is important to add that PtO formation proceeds concurrently with its dissolution. Thus, the amount of oxide formed at $E_p$ = 1.20 V for a given $t_p$ determined through its reduction by applying a negative-going CV transient corresponds to the amount of oxide remaining on the Pt surface. Thus, the actual amount of oxide that is formed equals the amount determined


DOI: 10.1021/cs5016035
ACS Catal. 2015, 5, 2605−2614

through its reduction plus the amount dissolved. Because at the present time there are no detailed kinetic data for Pt oxide dissolution as a function of $E_p$ and $t_p$, determination of the actual oxide that forms and includes the amount that is dissolved is impossible.

**Platinum Dissolution in Aqueous $HClO_4$ Solutions of Different Concentrations.** In an effort to understand the influence of pH on Pt dissolution, we analyzed the process in $HClO_4$, thus in an electrolyte containing a nonadsorbing or weekly adsorbing anion. Figure 7 presents CV profiles for a Pt

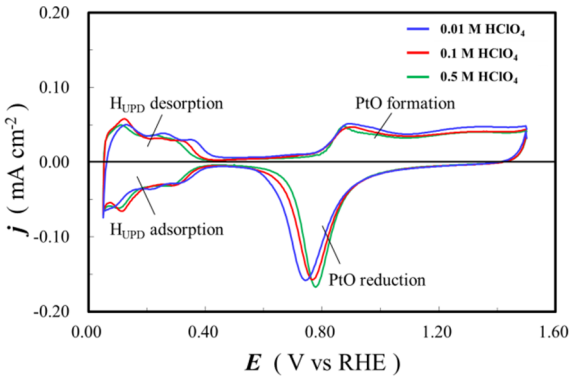


**Figure 7.** CV profiles for a Pt polycrystalline electrode obtained at $s$ = 50 mV $s^{-1}$ and $T$ = 293 K in aqueous $HClO_4$ solutions of different molar concentrations; $c$ = 0.01 M (blue line), 0.1 M (red line), and 0.5 M (green line).

polycrystalline electrode obtained at $s$ = 50 mV $s^{-1}$ and $T$ = 293 K in aqueous $HClO_4$ solutions of different concentrations, namely, $c$ = 0.01 M (blue line), 0.1 M (red line), and 0.5 M (green line). As the electrolyte concentration increases, the CV features associated with the electro-adsorption of $H_{UPD}$ shift toward less-positive potential values. On the other hand, the formation of PtO starts at almost the same potential but the PtO reduction peak shifts toward higher potentials.

Figure 8 presents the amount of dissolved Pt ($m_{Pt}$ in ng $cm^{-2}$) versus the potential switch cycle number ($n$) for repetitive potential switching and holding between 0.60 and 1.20 V at $T$ = 293 K in $c$ = 0.01 M (blue diamonds), 0.1 M (red diamonds), and 0.5 M (green diamonds) aqueous $HClO_4$ solutions. The amount of dissolved Pt is cumulative and refers

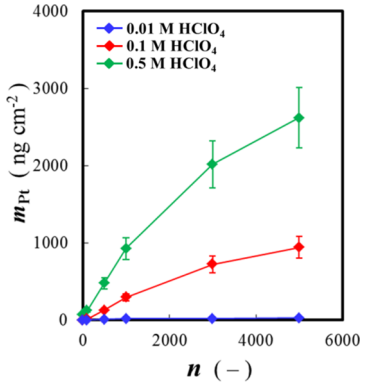


**Figure 8.** Amount of dissolved Pt ($m_{Pt}$) versus the potential switch cycle number ($n$) for repetitive potential switching and holding between 0.60 and 1.20 V at $T$ = 293 K in 0.01 M (blue diamonds), 0.1 M (red diamonds), and 0.5 M (green diamonds) aqueous $HClO_4$ solutions.

to the total amount in the electrolyte solutions. The results demonstrate that the amount of dissolved Pt increases by about 2 orders of magnitude with a 50-fold rise in the $HClO_4$ concentration; for $n$ = 5000 cycles, $m_{Pt}$ = 25 ± 3 ng $cm^{-2}$ in 0.01 M $HClO_4$ solution; $m_{Pt}$ = 941 ± 98 ng $cm^{-2}$ in 0.1 M $HClO_4$ solution; and $m_{Pt}$ = 2620 ± 390 ng $cm^{-2}$ in 0.5 M $HClO_4$ solution. These important results clearly demonstrate that the activity of proton has a significant impact on Pt dissolution. It is interesting to observe that the $m_{Pt}$ versus $n$ plots in Figure 8 are nonlinear. Bearing in mind that each potential switching and holding cycle generates the same amount of dissolved Pt, one would expect these plots to be linear. The nonlinearity is assigned to simultaneously occurring Pt electrodeposition as explained elsewhere.[13]

We also analyzed the influence of $HClO_4$ concentration on the Pt surface oxide formation in order to determine whether the amount of dissolved Pt correlates with the amount of Pt surface oxide. Figure 9 presents $q_{ox}$ versus log $t_p$ plots for Pt

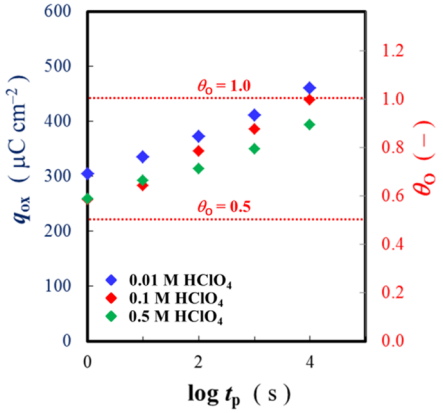


**Figure 9.** Oxide charge density ($q_{ox}$) versus log $t_p$ plots for Pt surface oxide growth at $E_p$ = 1.20 V and $T$ = 293 K in 0.01 M (blue diamonds), 0.1 M (red diamonds), and 0.5 M (green diamonds) aqueous $HClO_4$ solutions.

oxide growth at $E_p$ = 1.20 V in aqueous $HClO_4$ solutions of three different concentrations, namely, $c$ = 0.01 M (blue diamonds), 0.1 M (red diamonds), and 0.5 M (green diamonds). As expected, for a given concentration of $HClO_4$, the values of $q_{ox}$ increase with increasing $t_p$. In addition, for a given $t_p$ the values of $q_{ox}$ decrease with increasing $HClO_4$ concentration, and the difference is in the 10−15% range. The decrease in the amount of PtO as the concentration of $HClO_4$ increases could be related to concurrently occurring chemical dissolution of anodically formed PtO (a chemical reaction following an electrochemical reaction); the process involves protons as a reactant. Thus, the longest $t_p$ and the lowest acid concentration generate the thickest Pt oxide layer. Above, we demonstrate that the anion nature and concentration do not affect the surface oxide growth behavior. Consequently, we propose that the differences reported in Figure 9 are due to the change in proton concentration (pH change).

**Influence of the Anion Nature, Electrolyte pH, and Activity of $Pt^{z+}$ on Platinum Dissolution.** Our results presented above demonstrate that in the case of 0.1 M $CF_3SO_3H$, 0.1 M $H_2SO_4$, and 0.1 M $HClO_4$ solutions the amount of dissolved Pt is practically the same, whereas in the case of 0.5 M $H_2SO_4$ solution the amount of dissolved Pt is significantly greater than in 0.5 M $CF_3SO_3H$ and 0.5 M $HClO_4$


DOI: 10.1021/cs5016035
ACS Catal. 2015, 5, 2605−2614

solutions (Figure 3). Our results also demonstrate that an addition of $H_2SO_4$ to 0.1 or 0.5 M $HClO_4$ solutions has practically no impact on Pt dissolution, although higher acidity (lower pH) increases the extent of the process (Figure 5). These observations suggest that higher dissolution of Pt in 0.5 M $H_2SO_4$ solution cannot be explained in terms of direct interaction of the anion with the Pt electrode surface but rather in terms equilibrium constants of $Pt^{2+}$- and $Pt^{4+}$-containing complex compounds that the process produces. The nature of these compounds cannot be easily analyzed using traditional inorganic methods due to their very low concentration.

Elsewhere,[13] 11 possible mechanisms of electrochemical and chemical Pt dissolution were proposed, and their feasibility was discussed. Direct anodic dissolution of Pt to $Pt^{2+}$ or $Pt^{4+}$ proceeds without any involvement of the $H^+$ cation; thus, the respective processes do not depend on the electrolyte pH. However, anodic dissolution of PtO (prior to or after the structural transformation), cathodic dissolution of $PtO_2$, and chemical dissolution of PtO and $PtO_2$ involves the $H^+$ cation as a reactant; thus, the respective processes depend on the electrolyte pH.

The amount of dissolved Pt formed upon potential cycling was reported to be higher than that formed upon potential holding.[15] This behavior could be explained in terms of the number of oxide formation and reduction cycles which involve repetitive structural transformations (formation of $PtO_{quasi\text{-}3D\ lattice}$ and its reductive conversion to Pt). However, potential holding facilitates the establishing of equilibrium, while potential cycling does not. Recent ion-exchange chromatography coupled to inductively coupled plasma mass spectrometry (IEC-ICP-MS) measurements reveal that cycling in the 0.60−1.20 V range through the application of triangle-shaped potential versus time profile generates both $Pt^{2+}(aq)$ and $Pt^{4+}(aq)$ species, with at least 80% of electro-dissolved Pt being present as $Pt^{2+}$ complexes. These results suggest that at least two dissolution mechanisms producing two different dissolved species are operational.

As described elsewhere,[13] the upper potential limit ($E_U$) has a significant impact on the amount of dissolved Pt, especially as it exceeds the potential range in which the structural transformation from $O_{chem}$ to $PtO_{quasi\text{-}3D\ lattice}$ takes place ($1.10 \le E_U \le 1.20$ V). In the case of repetitive potential switching between 0.60 and 1.20 V with the potential measured versus RHE, 1.20 V on the RHE scale corresponds to 1.20 V on the SHE scale *only* if the activity of proton equals one ($a_{H^+} = 1.00$). However, if the activity of proton is 1 order of magnitude lower ($a_{H^+} = 1.0 \times 10^{-1}$), then the potential of 1.20 V on the RHE scale corresponds to 1.141 V on the SHE scale. Thus, a change in the electrolyte pH from 0 ($a_{H^+} = 1.00$) to 2 ($a_{H^+} = 1.0 \times 10^{-2}$) translates to a change of $E_U$ from 1.20 to 1.082 V on the SHE scale. As explained elsewhere,[13] a change of $E_U$ from 1.10 to 1.20 V increases the amount of dissolved Pt by a factor of 3 for $n = 1000$, a factor of 4 for $n = 2000$, and a factor of 6 for $n = 5000$. Consequently, in order to evaluate the impact of $E_U$ and $E_L$ in potential switching (the present contribution) or potential cycling experiments (our past contribution[13]), it is necessary to relate their values to the standard potentials of the PtO(s)/Pt(s), $PtO_2$(s)/$Pt^{2+}$(aq), $Pt^{2+}$(aq)/Pt(s), and $Pt^{4+}$(aq)/Pt(s) redox couples with the objective of determining whether the dissolution of Pt or Pt oxide follows chemical and/or electrochemical mechanism.

Figure 10 presents three $E$ (on the SHE scale) versus pH diagrams (Pourbaix diagrams) for Pt in acidic aqueous media for $T = 298$ K;[44] the graphs A, B, and C refer to the activities of $Pt^{2+}(aq)$ ($a_{Pt^{2+}}$) and $Pt^{4+}(aq)$ ($a_{Pt^{4+}}$) being 1.00, $1.0 \times 10^{-6}$, and $1.0 \times 10^{-9}$, respectively. In each graph, the black solid sloping line represents the potential of the $1/2O_2(g) + 2H^+(aq) + 2e^- = H_2O(l)$ reaction (the oxygen reduction reaction, ORR). The solid brown line represents the potential of the following redox reaction as a function of pH:

$$PtO(s) + 2H^+(aq) + 2e^- \rightarrow Pt(s) + H_2O(l) \quad (1)$$

which is given by eq 2:

$$E = E^\circ - \frac{RT}{2F}\ln\frac{1}{a_{H^+}^2} = 0.980 - 0.0592 \times pH \quad (2)$$

where $E^\circ = 0.980$ V is the standard potential of this redox process;[45] the value of $E$ depends on the electrolyte pH. Equation 1 refers to the formation of bulk PtO, which can undergo subsequent chemical dissolution.[26] The dashed brown line represents the potential of the following redox reaction as a function of pH:

$$PtO_2(s) + 4H^+(aq) + 2e^- \rightarrow Pt^{2+}(aq) + 2H_2O(l) \quad (3)$$

which is given by eq 4:

$$E = E^\circ - \frac{RT}{2F}\ln\frac{a_{Pt^{2+}}}{a_{H^+}^4} = 0.837 - 0.0296\log a_{Pt^{2+}} - 0.118 \times pH \quad (4)$$

where $E^\circ = 0.837$ V is the standard potential of this redox process;[45] the value of $E$ depends on the electrolyte pH. This reaction represents cathodic dissolution of $PtO_2$ with the formation of $Pt^{2+}$ cation. The solid purple line represents the potential of the following redox reaction:

$$Pt^{2+}(aq) + 2e^- \rightarrow Pt(s) \quad (5)$$

which is given by eq 6:

$$E = E^\circ - \frac{RT}{2F}\ln\frac{1}{a_{Pt^{2+}}} = 1.188 + 0.0296\log a_{Pt^{2+}} \quad (6)$$

where $E^\circ = 1.188$ V is the standard potential of this redox process (it refers to $a_{Pt^{2+}} = 1.00$);[45] its value does not depend on the electrolyte pH and only on the activity (concentration) of the $Pt^{2+}(aq)$ cation. The solid green line represents the potential of the following redox reaction:

$$Pt^{4+}(aq) + 4e^- \rightarrow Pt(s) \quad (7)$$

which is given by eq 8:

$$E = E^\circ - \frac{RT}{4F}\ln\frac{1}{a_{Pt^{4+}}} = 1.150 + 0.0148\log a_{Pt^{4+}} \quad (8)$$

where $E^\circ = 1.150$ V is the standard potential of this redox process (it refers to $a_{Pt^{4+}} = 1.00$);[45] its value does not depend on the electrolyte pH and only on the activity (concentration) of the $Pt^{4+}(aq)$ cation. The molal concentrations of $Pt^{2+}(aq)$ and $Pt^{4+}(aq)$ generated through Pt or Pt oxide dissolution are typically between $1.0 \times 10^{-9}$ and $1.0 \times 10^{-6}$ mol kg$^{-1}$ (at such low concentrations molality equals molarity).[13] Assuming that the mean activity coefficients of $Pt^{2+}(aq)$ and $Pt^{4+}(aq)$ equal unity ($\gamma_\pm = 1.00$; it is a reasonable assumption for a very diluted electrolyte), each 10-fold decrease in the $Pt^{2+}(aq)$ concentration reduces $E$ of the reaction depicted in eq 5 by 0.0296 V, and each 10-fold decrease in the $Pt^{4+}(aq)$ concentration reduces $E$ of the reaction depicted in eq 7 by 0.0148 V. Thus, in the case of $a_{Pt^{2+}} = 1.0 \times 10^{-6}$, $E = 1.010$ V (the graph B


DOI: 10.1021/cs5016035
ACS Catal. 2015, 5, 2605−2614

in Figure 10), and in the case of $a_{Pt^{2+}} = 1.0 \times 10^{-9}$, $E = 0.922$ V (the graph C in Figure 10) on the SHE scale. In the case of $a_{Pt^{4+}} = 1.0 \times 10^{-6}$, $E = 1.061$ V (the graph B in Figure 10), and in the case of $a_{Pt^{4+}} = 1.0 \times 10^{-9}$, $E = 1.017$ V on the SHE scale. The vertical green ($a_{H^+} = 1.00$, pH = 0), red ($a_{H^+} = 0.10$, pH = 1), and blue ($a_{H^+} = 0.010$, pH = 2) arrow-ended lines show the limits of the repetitive potential switching experiments but on the SHE scale. The changes in the values of $E_L$ and $E_U$ brought about by the modification of $a_{H^+}$ place them relative to the potential of the four redox couples discussed above (eqs 1, 3, 5, and 7). The graph A in Figure 10 refers to unrealistic conditions of $a_{Pt^{2+}} = 1.00$ and $a_{Pt^{4+}} = 1.00$. However, making an arbitrary assumption that such concentrations of dissolved $Pt^{2+}(aq)$ and $Pt^{4+}(aq)$ could be achieved and that $a_{H^+} = 1.00$ (pH = 0), potential cycling up to 1.20 V would still generate both $Pt^{2+}(aq)$ and $Pt^{4+}(aq)$ through direct anodic dissolution of metallic Pt. On the other hand, a decrease of $E_U$ to 1.10 V would not generate $Pt^{2+}(aq)$ or $Pt^{4+}(aq)$ through direct anodic dissolution of Pt. The graphs B ($a_{Pt^{2+}} = 1.0 \times 10^{-6}$ and $a_{Pt^{4+}} = 1.0 \times 10^{-6}$) and C ($a_{Pt^{2+}} = 1.0 \times 10^{-9}$ and $a_{Pt^{4+}} = 1.0 \times 10^{-9}$) in Figure 10 refer to realistic conditions encountered during Pt dissolution experiments. The location of the solid and dashed brown, purple, and green lines representing the potentials of the reactions depicted in eqs 1, 3, 5, and 7 with respect to the vertical, arrow-ended lines presenting the actual limits in the repetitive potential switching experiments reveal that all four reactions can actually take place. Thus, these four processes can occur and explain the formation of $Pt^{2+}(aq)$ and $Pt^{4+}(aq)$. It is important to emphasize that the PtO species in eq 1 is a bulk compound, while PtO formed upon potential switching or cycling is a surface species. The standard potential of the $PtO_{1\ ML,surf}/Pt_{surf}$ redox couple (eq 9; $PtO_{1\ ML,surf}$ refers to one monolayer of PtO residing on Pt surface) has never been defined, although it is well-established and widely accepted that PtO formation on polycrystalline Pt commences at 0.85 V and its reduction also commences also at 0.85 V.[20] Consequently, we adopt the potential of 0.85 V as an approximate standard potential of this surface redox.

$$PtO_{1ML,surf} + 2H^+(aq) + 2e^- \rightarrow Pt_{surf} + H_2O(l) \qquad (9)$$

Because this process involves two protons (as in eq 1), its potential is expected to decrease 0.0592 V with an increase of pH by 1. Because $PtO_{surf}$ develops through an anodic process at potential greater than 0.85 V, repetitive potential switching in the 0.60−1.20 V versus RHE range develops this species; it can undergo subsequent chemical dissolution. Similarly, the $PtO_2$ species in eq 3 is a bulk compound, while $PtO_2$ formed upon potential switching or cycling is a very thin layer of a surface compound. The standard potential of the $PtO_{2,surf}/Pt^{2+}$ redox couple (eq 3; $PtO_{2,surf}$ refers to a very thin surface layer of $PtO_2$) has never been defined or determined. Consequently, the adoption of the standard potential for $PtO_{2,bulk}/Pt^{2+}$ is the best assumption that may be made at the present time.

An analysis of the $E$ versus pH diagrams presented in panels B and C in Figure 10 reveals that the formation of $Pt^{2+}(aq)$ and $Pt^{4+}(aq)$ species with their respective activities being between $10^{-9}$ and $10^{-6}$ can be explained through the following: (i) direct anodic dissolution of Pt; (ii) chemical dissolution of anodically formed PtO; and (iii) cathodic dissolution of anodically formed $PtO_2$. Although there exists indisputable evidence for the existence of cathodic Pt oxide dissolution,[18,19] it is unclear whether $PtO_2$ can develop upon potential switching or cycling in the 0.60−1.20 V range. In addition, a large fraction

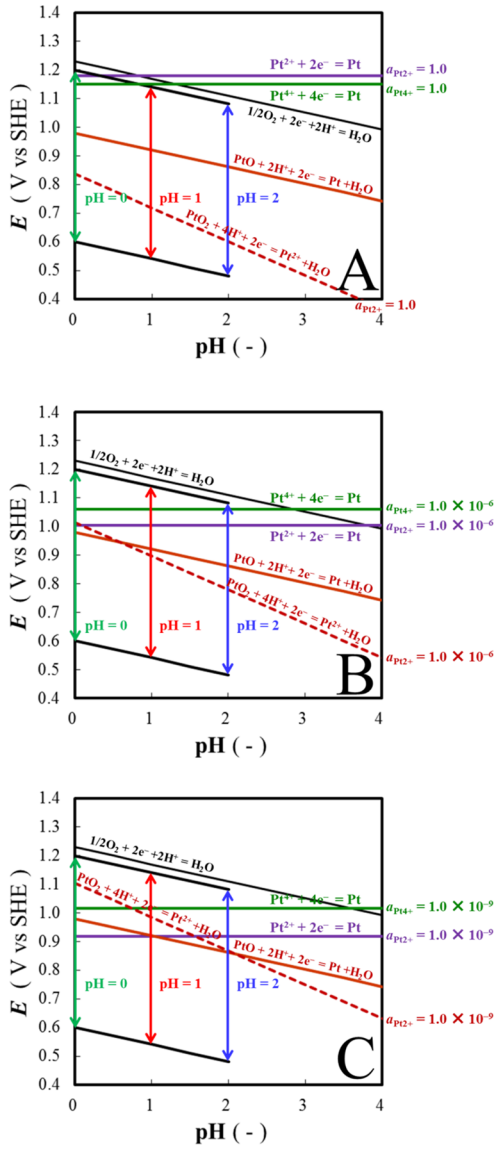


**Figure 10.** Three $E$ versus pH diagrams (Pourbaix diagrams) for Pt in aqueous acidic media for $T = 298$ K. Panels A, B, and C refer to the activities of $Pt^{2+}(aq)$ ($a_{Pt^{2+}}$) and $Pt^{4+}(aq)$ ($a_{Pt^{4+}}$) being 1.00, $1.0 \times 10^{-6}$, and $1.0 \times 10^{-9}$, respectively.

of cathodic dissolution is observed only in slow oxide-reduction transients, while in fast reduction experiments, the extent of anodic and cathodic dissolution is similar. Thus, in the case of square-wave potential versus time program, the experimentally observed dissolved Pt originates from both anodic and cathodic transients in addition to chemical dissolution of an anodically formed oxide. Consequently, it might be premature to assign the formation of $Pt^{2+}(aq)$ to the cathodic process depicted in eq 3, and a different cathodic process might have to be considered. Alternatively, indisputable evidence for the formation of $PtO_2$ upon application of $E_U = 1.20$ V should be provided in order to demonstrate that $Pt^{2+}$ can develop through cathodic dissolution of $PtO_2$.

Although the current contribution deals with Pt and Pt oxide dissolution in acidic media, it is important to discuss the process in alkaline solutions or acidic media doped with an additive. A recent comparative study of Pt dissolution in acidic and alkaline media demonstrates that the process also occurs in


DOI: 10.1021/cs5016035
ACS Catal. 2015, 5, 2605−2614

alkaline solutions.[46] Because an upper potential limit of 1.20 V on the RHE scale in aqueous electrolyte solution of pH = 14 (pOH = 0) would correspond to 0.37 V on the SHE scale, the formation of $Pt^{2+}$(aq) can only be explained through chemical dissolution of anodically formed PtO (there is no direct anodic dissolution of Pt). This finding indicates that chemical dissolution of PtO is an important process contributing to degradation of Pt materials. Another study on the stability of Pt electrocatalysts in aqueous formic acid solutions demonstrated that their degradation through dissolution phenomena was more significant (by a factor of 4−5) than under similar conditions but without formic acid being present.[47] These results combined with our findings show that Pt dissolution is a complex phenomenon that depends on several factors, such as potential conditions (cycling, switching, holding), electrolyte composition and pH, and temperature.

The Pourbaix diagrams presented in Figure 10 identify possible chemical and electrochemical reactions that can lead to Pt dissolution. By definition, they refer to stationary conditions, thus to conditions under which the potential experienced by Pt is constant and the solution pH does not change. In our experiments, the applied potential is held constant at $E_L$ = 0.60 V and $E_U$ = 1.20 V for $t$ = 3.0 s. Thus, the applied conditions are not strictly potentiostatic. Consequently, these Pourbaix diagrams serve as a useful first approximation but one should be careful in employing them to analyze data obtained under transient potential conditions. Finally, because the pH of the four electrolyte solutions falls in the 0.44−1.5 range, the pH range 0−4 covered in Figure 10 fits the qualitative analysis presented above.

## CONCLUSIONS

Electrochemical and chemical dissolution of polycrystalline Pt in aqueous $CF_3SO_3H$, $H_2SO_4$, and $HClO_4$ solutions of two different concentrations ($c$ = 0.1 and 0.5 M) was studied by means of inductively coupled plasma mass spectrometry. The dissolution of Pt was accomplished by repetitive potential switching and holding in the 0.60−1.20 V range and at a temperature of $T$ = 293 K. These conditions were selected because they simulate the real conditions encountered by catalyst layers of automotive polymer electrolyte membrane fuel cells. The contribution reports the first analysis of Pt degradation in aqueous $CF_3SO_3H$ solutions. Experimental work on Pt degradation in $CF_3SO_3H$ is of particular importance because the latter is the smallest fluorinated sulfonic acid and can serve as a suitable molecular model in evaluating the impact of anion on Pt dissolution. In the case of $c$ = 0.1 M aqueous $CF_3SO_3H$, $H_2SO_4$, and $HClO_4$ solutions, the amount of dissolved Pt is the same. However, in the case of $c$ = 0.5 M solutions, the amount of dissolved Pt in $CF_3SO_3H$ and $HClO_4$ is the same but significantly lower than that in $H_2SO_4$. The influence of anion nature and electrolyte pH on electrochemical and chemical Pt dissolution was also studied in 0.1 and 0.5 M $HClO_4$ without or with $1.0 \times 10^{-2}$ M $H_2SO_4$ addition. Because the addition of $H_2SO_4$ did not affect the amount of dissolved Pt, it is concluded that in the case of these two species the anion nature has no or negligible impact on the process. On the other hand, an increase in the electrolyte acidity (a decrease in pH) significantly enhances Pt dissolution. In order to better understand the dissolution of polycrystalline Pt brought about by potential switching and holding, potential versus pH diagrams (Pourbaix diagrams) for the 0.1 and 0.5 M acid solutions containing $Pt^{2+}$(aq) and $Pt^{4+}$(aq) cations of different activities ($a_{Pt^{2+}}$ = $1.0 \times 10^{-9}$, $1.0 \times 10^{-6}$, and 1.00; and $a_{Pt^{4+}}$ = $1.0 \times 10^{-9}$, $1.0 \times 10^{-6}$, and 1.00) were prepared. In addition, the lower and upper potential limits ($E_L$, $E_U$) measured versus RHE were converted to the SHE scale. An analysis of the potential and electrolyte pH conditions led to the observation that dissolved Pt present in the form of $Pt^{2+}$(aq) can develop through chemical dissolution of anodically formed PtO or through direct anodic dissolution of Pt. However, a comparison of results obtained in alkaline media suggests that the latter process can be excluded.[46] Dissolved Pt present in the form of $Pt^{4+}$(aq) can develop through cathodic dissolution of $PtO_2$ or direct anodic dissolution of Pt. The cathodic dissolution requires the presence of $PtO_2$, which for the time being has not been reported to form at potential up to 1.20 V. Because cathodic Pt dissolution undeniably exists, these findings call for further research on Pt electro-oxidation and dissolution through the application of complementary electrochemical, analytical chemistry, and surface science techniques. The experimental results and their analysis presented in this contribution show that electrochemical and chemical dissolution of Pt can be successfully studied using electrochemical and analytical techniques. Inductively coupled plasma mass spectrometry is of particular significance due to its high detection limit. The outcome of this research validates the above-described experimental approach and demonstrates its applicability to other transition metals and electrochemical systems.

## AUTHOR INFORMATION

### Corresponding Author

*E-mail: gregory.jerkiewicz@chem.queensu.ca. Tel.: (613) 5336413.

### Notes

The authors declare no competing financial interest.

## REFERENCES

(1) Ohma, A.; Mashio, T.; Sato, K.; Iden, H.; Ono, Y.; Sakai, K.; Akizuki, K.; Takaichi, S.; Shinohara, K. *Electrochim. Acta* **2011**, *56*, 10832−10841.

(2) Papageorgopoulos, D. Fuel Cells Overview. Presented at the U.S. Department of Energy (DOE) 2014 Fuel Cells Annual Merit Review, Washington DC, June 16−24, 2014. http://www.hydrogen.energy.gov/pdfs/review14/fc000_papageorgopoulos_2014_o.pdf (accessed August 1, 2014).

(3) Darling, R. M.; Meyers, J. P. *J. Electrochem. Soc.* **2003**, *150*, A1523−A1527.

(4) Darling, R. M.; Meyers, J. P. *J. Electrochem. Soc.* **2005**, *152*, A242−A247.

(5) Rinaldo, S. G.; Stumper, J.; Eikerling, M. *J. Phys. Chem. C* **2010**, *114*, 5773−5785.

(6) Rinaldo, S. G.; Lee, W.; Stumper, J.; Eikerling, M. *Electrochem. Solid-State Lett.* **2011**, *14*, B47−B49.

(7) Ahluwalia, R. K.; Arisetty, S.; Wang, X.; Wang, X.; Subbaraman, R.; Ball, S. C.; DeCrane, S.; Myers, D. J. *J. Electrochem. Soc.* **2013**, *160*, F447−F445.

(8) Ohma, A.; Shinohara, K.; Iiyama, A.; Yoshida, T.; Daimaru, A. *ECS Trans.* **2011**, *41*, 775−784.

(9) Aoyama, T.; Iiyama, A.; Shinohara, K.; Kamegaya, S.; Yamamoto, S.; Ban, Y. *SAE Int. J. Engines* **2009**, *1*, 314−323.

(10) Kongkanand, A.; Ziegelbauer, J. M. *J. Phys. Chem. C* **2012**, *116*, 3684−3693.

(11) Liu, Y.; Mathias, M.; Zhang, J. *Electrochem. Solid-State Lett.* **2010**, *13*, B1−B3.

(12) Tang, L.; Han, B.; Persson, K.; Friesen, C.; He, T.; Sieradzki, K.; Ceder, G. *J. Am. Chem. Soc.* **2010**, *132*, 596−600.



DOI: 10.1021/cs5016035
*ACS Catal.* 2015, 5, 2605−2614

(13) Xing, L.; Hossain, M. A.; Tian, M.; Beauchemin, D.; Adjemian, K. T.; Jerkiewicz, G. *Electrocatalysis* **2014**, *5*, 96−112.
(14) Uchimura, M.; Kocha, S. *ECS Trans.* **2007**, *11*, 1215−1226.
(15) Wang, X.; Kumar, R.; Myers, D. J. *Electrochem. Solid-State Lett.* **2006**, *9*, A225−A227.
(16) Matsumoto, M.; Miyazaki, T.; Imai, H. *J. Phys. Chem. C* **2011**, *115*, 11163−11169.
(17) Sugawara, Y.; Okayasu, T.; Yadav, A. P.; Nishikata, A.; Tooru, T. *J. Electrochem. Soc.* **2012**, *159*, F779−F786.
(18) Topalov, A. A.; Katsounaros, I.; Auinger, M.; Cherevko, S.; Meier, J. C.; Klemm, S. O.; Mayrhofer, K. J. J. *Angew. Chem., Int. Ed.* **2012**, *51*, 12613−12615.
(19) Topalov, A. A.; Cherevko, S.; Zeradjanin, A. R.; Meier, J. C.; Katsounaros, I.; Mayrhofer, K. J. J. *Chem. Sci.* **2014**, *5*, 631−638.
(20) Jerkiewicz, G.; Vatankhah, G.; Lessard, J.; Soriaga, M.; Park, Y.-S. *Electrochim. Acta* **2004**, *49*, 1451−1459.
(21) Conway, B. E.; Barnett, B.; Angerstein-Kozlowska, H.; Tilak, B. V. *J. Chem. Phys.* **1990**, *93*, 8361−8373.
(22) Hiraoka, F.; Matsuzawa, K.; Shigenori, M. *Electrocatalysis* **2012**, *4*, 10−16.
(23) Mitsushima, S.; Kawahara, S.; Ota, K.; Kamiya, N. *J. Electrochem. Soc.* **2007**, *154*, B153−B158.
(24) Cherevko, S.; Topalov, A. A.; Zeradjanin, A. R.; Keeley, G. P.; Mayrhofer, K. J. J. *Electrocatalysis* **2014**, *5*, 235−240.
(25) Topalov, A. A.; Zeradjanin, A. R.; Cherevko, S.; Mayrhofer, K. J. J. *Electrochem. Commun.* **2013**, *40*, 49−53.
(26) Mitsushima, S.; Koizumi, Y.; Uzuka, S.; Ota, K. *Electrochim. Acta* **2008**, *54*, 455−460.
(27) Yadav, A. P.; Okayasu, T.; Sugawara, Y.; Nishikata, A.; Tsuru, T. *J. Electrochem. Soc.* **2012**, *159*, C190−C194.
(28) Komanicky, V.; Chang, K. C.; Menzel, A.; Markovic, N. M.; You, H.; Wang, X.; Myers, D. *J. Electrochem. Soc.* **2006**, *153*, B446−B451.
(29) Subbaraman, R.; Strmcnik, D.; Stamenkovic, V.; Markovic, N. M. *J. Phys. Chem. C* **2010**, *114*, 8414−8422.
(30) Hanawa, H.; Kunimatsu, K.; Watanabe, M.; Uchida, H. *J. Phys. Chem. C* **2012**, *116*, 21401−21406.
(31) Kodama, K.; Jinnouchi, R.; Suzuki, T.; Murata, H.; Hatanaka, T.; Morimoto, Y. *Electrochem. Commun.* **2013**, *36*, 26−28.
(32) Masuda, T.; Sonsudin, F.; Singh, P. R.; Naohara, H.; Uosaki, K. *J. Phys. Chem. C* **2013**, *117*, 15704−15709.
(33) Ohma, A.; Fushinobu, K.; Okazaki, K. *Electrochim. Acta* **2010**, *55*, 8829−8839.
(34) Attard, G.; Brew, A.; Hunter, K.; Sharman, J.; Wright, E. *Phys. Chem. Chem. Phys.* **2014**, *16*, 13689−13698.
(35) Ohma, A.; Ichiya, T.; Fushinobu, K.; Okazaki, K. *Surf. Sci.* **2010**, *604*, 965−973.
(36) Teliska, M.; Murthi, V.; Mukerjee, S.; Ramaker, D. E. *J. Phys. Chem. C* **2007**, *111*, 9267−9274.
(37) Berna, A.; Feliu, J. M.; Gancs, L.; Mukerjee, S. *Electrochem. Commun.* **2008**, *10*, 1695−1698.
(38) Hsueh, K.-L.; Chang, H. H.; Chin, D.-T.; Srinivasan, S. *Electrochim. Acta* **1985**, *30*, 1137−1142.
(39) Kodama, K.; Shinohara, A.; Hasegawa, N.; Shinozaki, K.; Jinnouchi, R.; Suzuki, T.; Hatanaka, T.; Morimoto, Y. *J. Electrochem. Soc.* **2014**, *161*, F649−F652.
(40) Chen, D.; Tao, Q.; Liao, L. W.; Liu, S. X.; Chen, Y. X.; Ye, S. *Electrocatalysis* **2011**, *2*, 207−219.
(41) Conway, B. E.; Angerstein-Kozlowska, H.; Sharp, W. A.; Criddle, E. E. *Anal. Chem.* **1973**, *45*, 1331−1336.
(42) Alsabet, M.; Grden, M.; Jerkiewicz, G. *J. Electroanal. Chem.* **2006**, *589*, 120−127.
(43) Zolfaghari, A.; Chayer, M.; Jerkiewicz, G. *J. Electrochem. Soc.* **1997**, *144*, 3034−3041.
(44) Pourbaix, M. J. N.; Muylder, J. Van; Zoubov, N. de. *Platin. Met. Rev.* **1959**, *3*, 47−53.
(45) *Standard Potentials in Aqueous Solution*; Bard, A. J., Parsons, R., Eds.; Marcel Dekker: New York, 1985.
(46) Cherevko, S.; Zeradjanin, A. R.; Keeley, G. P.; Mayrhofer, K. J. J. *J. Electrochem. Soc.* **2014**, *161*, H822−H830.
(47) Fayette, M.; Nutariya, J.; Vasiljevic, N.; Dimitrov, N. *ACS Catal.* **2013**, *3*, 1709−1718.


DOI: 10.1021/cs5016035
*ACS Catal.* 2015, 5, 2605−2614